International Journal of Nanoparticles

ISSN online: 1753-2515 - ISSN print: 1753-2507
https://www.inderscience.com/ijnp

Influence of particle size on optical scattering properties of silver nanoparticles

Ayoub Lamsiah, El Houssine Atmani, Jaafar Meziane, Nejma Fazouan, Maria Oumouloud

DOI: 10.1504/IJNP.2026.10075618

Article History:

Received:	30 December 2024
Last revised:	23 October 2025
Accepted:	24 October 2025
Published online:	19 January 2026

Influence of particle size on optical scattering properties of silver nanoparticles

Ayoub Lamsiah*, El Houssine Atmani, Jaafar Meziane, Nejma Fazouan and Maria Oumouloud

Laboratory of Nanostructures and Advanced Materials, Mechanics and Thermofluids,
FST Mohammedia,
Hassan II University of Casablanca, Morocco
and
Laboratory of Materials, Energy and System Control,
FST Mohammedia,
Hassan II University of Casablanca, Morocco
Email: lamsiahayoub@gmail.com
Email: eh5atmani@gmail.com
Email: jaafar.meziane@univh2c.ma
Email: nejma.fazouan@univh2c.ma
Email: maria.oumouloud@univh2c.ma
*Corresponding author

Abstract: Nanometric metallic particles have attracted considerable attention due to their wide-ranging applications in healthcare, renewable energy, and other advanced technologies, stemming from their distinctive physical and chemical properties. These nanoparticles can enhance the efficiency of solar cells and act as biological markers in cancer diagnostics and therapy. The light-scattering behaviour of metallic nanoparticles is highly dependent on parameters such as particle size, composition, shape, and the surrounding medium. In this work, we examine how the size of silver nanoparticles influences light-scattering phenomena. Using the Lorentz-Drude model, we compute the absorption, scattering, and extinction cross-sections. By analysing optical efficiency across different incident light wavelengths, we interpret the computational outcomes and discuss their physical significance.

Keywords: silver nanoparticles size; light scattering; scattering cross section; Lorentz-Drude model; optical efficiency.

Reference to this paper should be made as follows: Lamsiah, A., Atmani, E.H., Meziane, J., Fazouan, N. and Oumouloud, M. (2026) 'Influence of particle size on optical scattering properties of silver nanoparticles', *Int. J. Nanoparticles*, Vol. 15, No. 5, pp.1–17.

Biographical notes: Ayoub Lamsiah is a Doctor at the Laboratory of Mathematics and Physical Sciences Applied to Engineering Sciences, Faculty of Sciences and Technologies, Hassan II University of Casablanca, and a radiology technician at a public hospital. Her academic and research interests include medical physics, nanomaterials and light-matter interaction, with emphasis on imaging techniques and modelling. Her strategic research axes include energy, advanced materials, medical applications, and mechanics.

El Houssine Atmani is a Full Professor of Physics at the Department of Physics, Faculty of Sciences and Techniques de Mohammedia, Hassan II University of Casablanca, and Vice-Dean for Academic Affairs at the Faculty. He also directs research activities in the mathematics and applied physical sciences for engineering research unit. His research interests include materials physics, energy conversion, renewable energies and mechanics, with emphasis on experimental and theoretical methods in applied physics and engineering sciences. His strategic research axes include energy, advanced materials and mechanics.

Jaafar Meziane is a Full Professor at the Department of Physics, Faculty of Sciences and Technologies, Hassan II University of Casablanca, and a member of the Laboratory of Materials, Energy and System Control (FST Mohammedia). His research interests lie in theoretical and applied physics, with particular focus on materials physics, energy research, and mechanics. He has contributed to curriculum development and supervised student research in areas such as condensed matter, optical phenomena, and energy systems. His strategic research axes include energy, advanced materials, and mechanics.

Nejma Fazouan is a Full Professor at the Department of Physics, Faculty of Sciences and Techniques de Mohammedia, Hassan II University of Casablanca, and member of the Mathematics and Applied Physical Sciences for Engineering Research Unit, where her work includes advanced materials and energy-related research. She serves on departmental scientific and pedagogical committees and coordinates graduate programmes. Her research interests focus on materials physics, energy, mechanics, and modelling of physical systems. Her strategic research axes include energy, advanced materials, and mechanics.

Maria Oumouloud is a high school teacher of physics and chemistry and a PhD student at the Laboratory of Mathematics and Physical Sciences Applied to Engineering Sciences, Faculty of Sciences and Technologies, Hassan II University of Casablanca. Her academic and research interests include medical physics, nanomaterials and light-matter interaction, with emphasis on optical scattering and modelling. Her strategic research axes include energy, advanced materials, medical applications, and mechanics.

1 Introduction

Recent studies have increasingly focused on exploring the electronic and magnetic properties of nanoparticles across diverse domains such as astrophysics, medical diagnostics and therapy, and nuclear waste management. Key parameters used to numerically characterise silver nanomaterials include the refractive index, permittivity, permeability, and dielectric conductivity (Fowler, 2008). Although a single-value dielectric function can be employed, our simulations utilise the Lorentz–Drude model database, which provides wavelength-dependent complex dielectric functions. This approach enhances both the accuracy and numerical convergence of the results (Sehmi et al., 2017; Gouesbet and Gréhan, 2011).

In recent years, remarkable progress has been achieved in the synthesis and applications of silver nanoparticles (AgNPs), not only because of their exceptional optical properties but also due to their versatility in fields ranging from diagnostics and catalysis to energy conversion and environmental monitoring (Mali et al., 2024; Amirjani et al.,

2023; Hang et al., 2024). These developments have underscored the crucial role of size-dependent optical behaviour, motivating extensive experimental and theoretical investigations aimed at optimising particle performance across different spectral regions (Yilmaz et al., 2022; Ishfaq et al., 2022).

Beyond conventional models, recent research has revealed the significance of quantum-size and nonlocal effects, particularly in nanoparticles smaller than 20 nm, where classical theories fail to accurately predict resonance features (Zhuo et al., 2021; Derkachova and Kolwas, 2021; Liu et al., 2021). These findings emphasise the need for hybrid models that bridge classical electrodynamics and quantum confinement effects.

Advanced numerical approaches have also been extensively applied to better understand the plasmonic behaviour of silver nanoparticles. Amirjani and Sadrnezhaad (2021) demonstrated that computational electromagnetics is a robust method for analysing the optical response of plasmonic nanostructures. Furthermore, Amirjani et al. (2020) showed that the particle size of silver nanoparticles can be predicted from their optical properties, confirming the strong dependence of plasmonic behaviour on size. Additionally, finite and boundary element methods have enabled highly accurate simulations of optical responses (Amirjani et al., 2022). Collectively, these studies highlight the critical role of nanoparticle size in the scattering of electromagnetic waves, thereby supporting the focus of the present investigation.

The Lorentz–Drude model enables calculation of the wavelength-dependent dielectric function or refractive index, expressed in terms of its real and imaginary components, $\varepsilon_i = n_i + *k_i$.

We consider a linearly polarised plane electromagnetic wave incident perpendicularly to the propagation direction (Bohren and Huffman, 2008). The nanoparticles are assumed to be spherical, with radii ranging from 5 nm to 120 nm.

Mie theory is employed to analyse the scattering of electromagnetic waves by spherical silver nanoparticles. It provides analytical expressions for electromagnetic and optical parameters, including internal and external scattering coefficients, as well as scattering, absorption, and extinction cross-sections, all as functions of wavelength (Wiscombe, 1980).

However, for extremely small nanoparticles (below approximately 10 nm), the classical local models – such as Lorentz–Drude combined with Mie theory – become inadequate. Nonlocal effects and quantum-size corrections can substantially alter the optical response, necessitating more sophisticated modelling frameworks (Zhuo et al., 2021). Furthermore, complex morphologies such as core–shell or metal–dielectric hybrid nanoparticles offer additional tunability of plasmonic resonances that cannot be captured by homogeneous sphere models. Recent investigations have demonstrated how such geometries allow precise control over scattering and absorption characteristics for applications in photovoltaics, sensing, and biomedical imaging (Ishfaq et al., 2022; Yang et al., 2020). Although the present study focuses on homogeneous spherical silver nanoparticles, future extensions of our model will aim to incorporate these nonlocal effects and complex geometries to better reflect real-world systems.

2 Methodology

2.1 Analytical formulation of Mie theory

Several theoretical frameworks, most notably Mie theory, are employed to analyse the scattering of electromagnetic waves by spherical silver nanoparticles. Mie theory offers analytical solutions for both electromagnetic and optical parameters, including internal and external scattering coefficients, as well as the scattering, absorption, and extinction cross-sections, each expressed as a function of wavelength (Wiscombe, 1980). The analytical formulation of Mie theory entails rigorous mathematical and physical derivations. The scalar wave equation in spherical coordinates can be expressed as:

$$\frac{1}{r^2}\frac{\partial}{\partial r}\left(r^2\frac{\partial\psi}{\partial r}\right)+\frac{1}{r^2 sin(\theta)}\frac{\partial}{\partial\theta}\left(sin(\theta)\frac{\partial\psi}{\partial\theta}\right)+\frac{1}{r^2 sin(\theta)}\frac{\partial^2\psi}{\partial\phi^2}+k^2m^2\psi=0 \quad (1)$$

To solve the scalar wave equation in spherical coordinates, the method of separation of variables is applied. By substituting the following functional form into the preceding equation:

$$\frac{1}{r^2}\frac{1}{R}\frac{\partial R}{\partial r}\left(r^2\frac{\partial R}{\partial r}\right)+\frac{1}{r^2 sin(\theta)}\frac{1}{\Theta}\frac{\partial}{\partial\theta}\left(sin(\theta)\frac{\partial\Theta}{\partial\theta}\right)+\frac{1}{r^2 sin(\theta)}\frac{1}{\Phi}\frac{\partial^2\Phi}{\partial\phi^2}+k^2m^2=0 \quad (2)$$

By multiplying both sides of the equation by $r^2sin^2(\theta)$, it can be rewritten in the following form:

$$sin^2(\theta)\frac{1}{R}\frac{\partial R}{\partial r}\left(r^2\frac{\partial R}{\partial r}\right)+sin(\theta)\frac{1}{\Theta}\frac{\partial}{\partial\theta}\left(sin(\theta)\frac{\partial\Theta}{\partial\theta}\right)+k^2m^2r^2sin^2(\theta)+\frac{1}{\Phi}\frac{\partial^2\Phi}{\partial\phi^2}+=0 \quad (3)$$

Hence, the general solution to the above equation can be expressed as:

$$r\psi(r,\theta,\phi)=\sum_{n=0}^{\infty}\sum_{l=-n}^{n}p_n^l\left(cos(\theta)\left[C_n\psi_n(kmr)+d_n\chi_n(kmr)\right]\left(a_l cos(l\phi)+b_l sin(l\phi)\right)\right) \quad (4)$$

Since $\psi_n(kr)$ represents the transmitted internal wave, which exhibits a singularity at the origin, a numerical series expansion is employed. This approach allows the wave function to be expressed as follows:

$$ru^t=\frac{1}{mk}\sum_{n=1}^{\infty}(-i)^n\frac{2n+1}{n(n+1)}C_n\psi_n(kr)p_n^l(cos(\theta)cos(\phi)), \quad (5)$$

$$rv^t=\frac{1}{k}\sum_{n=1}^{\infty}(-i)^n\frac{2n+1}{n(n+1)}d_n\psi_n(kr)p_n^l(cos(\theta)cos(\phi)), \quad (6)$$

Hankel Hankel functions are employed to represent the scattered wave. The functions $\chi_n(kr)$ and $\psi_n(kr)$ possess the desirable property of vanishing at infinity, thereby ensuring that the boundary conditions are physically satisfied.

$$ru^d = \frac{1}{k}\sum_{n=1}^{\infty}(-i)^n \frac{2n+1}{n(n+1)} a_n \xi_n(kr) p_n^l(cos(\theta)cos(\phi)) \tag{7}$$

$$rv^d = \frac{1}{k}\sum_{n=1}^{\infty}(-i)^n \frac{2n+1}{n(n+1)} b_n \xi_n(kr) p_n^l(cos(\theta)sin(\phi))$$

The internal scattering coefficients for silver nanoparticles are expressed as follows:

$$a_n = \frac{\psi_n'(y)\psi_n(x) - m\psi_n(y)\psi_n'(x)}{\psi_n'(y)\zeta_n(x) - m\psi_n(y)\zeta_n'(x)}, \tag{9}$$

$$b_n = \frac{\psi_n'(y)\psi_n(x) - m\psi_n(y)\psi_n'(x)}{\psi_n'(y)\zeta_n(x) - m\psi_n(y)\zeta_n'(x)}, \tag{10}$$

By substituting the expressions for the internal scattering coefficients into the preceding equations and performing the necessary mathematical manipulations, the following expressions for the absorption, scattering, and extinction cross-sections are obtained:

The scattering cross-section, denoted as c_{sca}, is defined as

$$c_{sca} = \frac{W_{sca}}{I_i} = \frac{2\pi}{k^2}\sum_{n=1}^{\infty}(2n+1)\left(|a_n|^2 + |b_n|^2\right) \tag{11}$$

The extinction cross-section is expressed as:

$$c_{ext} = \frac{W_{ex}}{I_i} = \frac{2\pi}{k^2}\sum_{n=1}^{\infty}(2n+1)Re\left(a_n + b_n\right) \tag{12}$$

The absorption cross-section is expressed as:

$$c_{abs} = c_{ext} - c_{sca} \tag{13}$$

2.2 Order and uncertainties of Mie theory

Light scattering by silver nanoparticles was modelled using the complete Mie theory, with the multipole expansion truncated at order N:

$$\left(N = \left\lceil x + 4.05x^{\frac{1}{3}} + 2 \right\rceil\right)$$

where $\left(x = \frac{2\pi R}{\lambda}\right)$ is the size parameter.

For the particle radii investigated (5–120 nm) within the visible spectral range (300–800 nm), the maximum number of terms required is approximately ($N \approx 12$). His truncation ensures numerical convergence of the extinction and scattering cross-sections with an uncertainty below 10^{-3}.

The dielectric function of silver was modelled using the Lorentz–Drude formulation, with parameters fitted from bulk optical data. For nanoparticles with radii smaller than 10 nm, a surface-damping correction $\gamma_{eff} = \gamma_{bulk} + Av_F/R$ was applied to account for electron–surface scattering.

The principal limitations of this model arise from the use of bulk parameters in the nanometric regime, the neglect of nonlocal and quantum effects for (R ≤ 5 nm), and the assumption of perfectly spherical, isolated particles. These factors may introduce typical uncertainties of 5–20 % in simulated intensities and spectral shifts of up to 10–30 nm in the plasmon-resonance position.

The truncation order of the Mie series adopted in this study was set to a fixed number of terms, ensuring convergence; however, numerical inaccuracies can still occur if the order is insufficient. Future investigations will examine the sensitivity of the results to the chosen truncation order and test alternative convergence criteria.

To further refine model parameters and improve Mie-series convergence, recent studies have introduced optimised fitting techniques and corrected formulations of the Lorentz–Mie framework (Fujii, 2014; Klinavičius et al., 2024; Rahimzadegan et al., 2020). These approaches reduce numerical artefacts and provide closer agreement with experimental spectra, particularly for broad resonance regimes and higher-order scattering components.

To validate the reliability of the results obtained from combining the Lorentz–Drude model with Mie theory, we referred to well-established experimental works. In particular, the studies by Hlaing et al. (2016) and Kolwas et al. (2013) provide precise measurements of absorption, scattering, and extinction cross-sections for spherical silver nanoparticles across radii from 5 nm to 100 nm – exactly matching the range investigated here. These data enable direct comparison between our theoretical predictions and empirical trends, confirming the overall spectral behaviour observed experimentally.

3 Results and discussion

Using Mie theory, we calculated the extinction, absorption, and scattering cross-sections to investigate how nanoparticle radius influences their optical behaviour (Hao and Nordlander, 2007; Du, 2004). Employing the Lorentz–Drude model, we present in the following figures the wavelength-dependent variations of these cross-sections for silver nanoparticles with radii of r = 5, 20, 40, 60, 80, 100 and 120 nm. The data were obtained from the Lorentz–Drude model database, and all results are plotted on an algorithmic scale to ensure consistent visualisation of the magnitude differences among the various sizes.

For nanoparticles with a radius of 5 nm, the curves clearly indicate that the absorption cross-section is substantially greater than the scattering cross-section. The absorption peak appears around 350 nm, within the ultraviolet region. At this very small scale, nanoparticles act primarily as light absorbers, capturing incident energy rather than redirecting it. This corresponds to the quasi-static regime, in which the particle size is much smaller than the wavelength of incident light. In this context, scattering is almost negligible, and the extinction cross-section S_{abs}, i.e., $S_{ext} \approx S_{abs}$, with $S_{sca} \approx 0$. Such behaviour is desirable in applications that require strong absorption, including optical heating systems and contrast agents for biomedical imaging.

$$s_{ext} = 1,0.10^{-13}; s_{abs} = 0,98.10^{-13}; s_{sca} = 0,02.10^{-13}$$

It is important to emphasise that the calculations presented in this study are based on classical models – specifically, the Lorentz–Drude formulation combined with Mie

theory – which do not account for several critical physical phenomena that arise at the nanoscale. For particles with radii smaller than 20 nm, quantum confinement effects and electron–surface scattering can significantly modify the complex permittivity of silver. These effects alter the electronic density of states and the overall optical response of the material, leading to deviations from classical predictions, particularly in plasmonic resonance positions and absorption intensities. In the absence of such corrections, theoretical estimates for the smallest nanoparticles may either overestimate or underestimate specific optical parameters, such as absorption or extinction. Recent studies (Derkachova and Kolwas, 2021; Zhuo et al., 2021) have demonstrated that incorporating nonlocal models or quantum corrections produces spectra that more closely reproduce experimental data for particles smaller than approximately 10–15 nm. Therefore, to enhance the predictive accuracy in this size regime, future extensions of the present work should employ hybrid models that integrate these quantum and nonlocal effects.

Figure 1 Scattering, extinction, and absorption cross-section for r = 5 nm (see online version for colours)

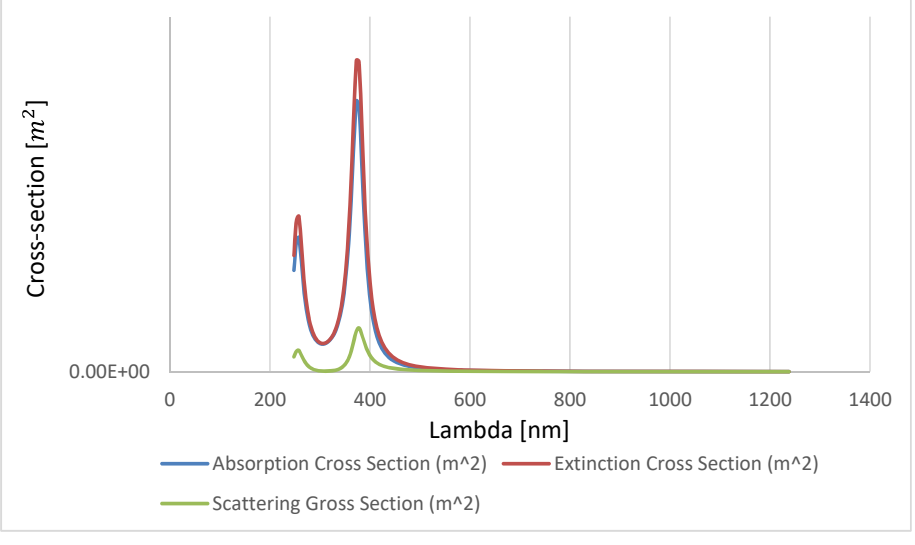

The results obtained for nanoparticles with radius r = 20 nm, are shown in Figure 2. As the radius increases to this value, the curves exhibit a pronounced rise in the scattering component. The absorption peak broadens and shifts slightly toward longer wavelengths, reaching approximately 500 nm, near the centre of the visible spectrum. At this scale, nanoparticles begin to scatter light appreciably, although absorption remains marginally dominant. The extinction cross-section S_{ext}, defined as the sum of S_{abs} + S_{sca}, increases accordingly. This behaviour signifies a transition toward a more complex interaction regime in which incident light is both absorbed and redirected. Such dual absorption scattering characteristics are particularly advantageous for optical technologies such as plasmonic sensors and visible-light photocatalysts.

$$s_{ext} = s_{sca} + s_{abs}; s_{ext} = 6,5.10^{-14}; s_{abs} = 4,0.10^{-14}; s_{sca} = 2,5.10^{-14}$$

Figure 2 Scattering, extinction, and absorption cross-section for r = 20 nm (see online version for colours)

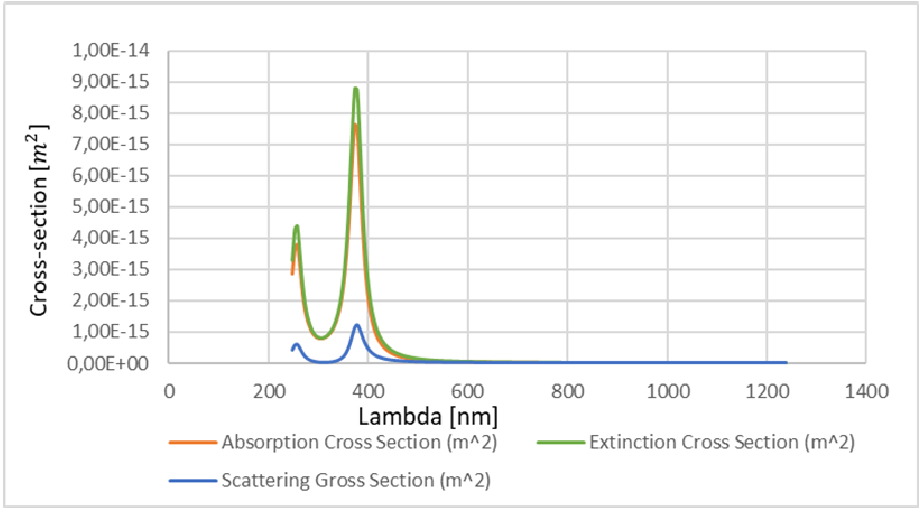

Figure 3 Scattering, extinction, and absorption cross-section for r = 50 nm (see online version for colours)

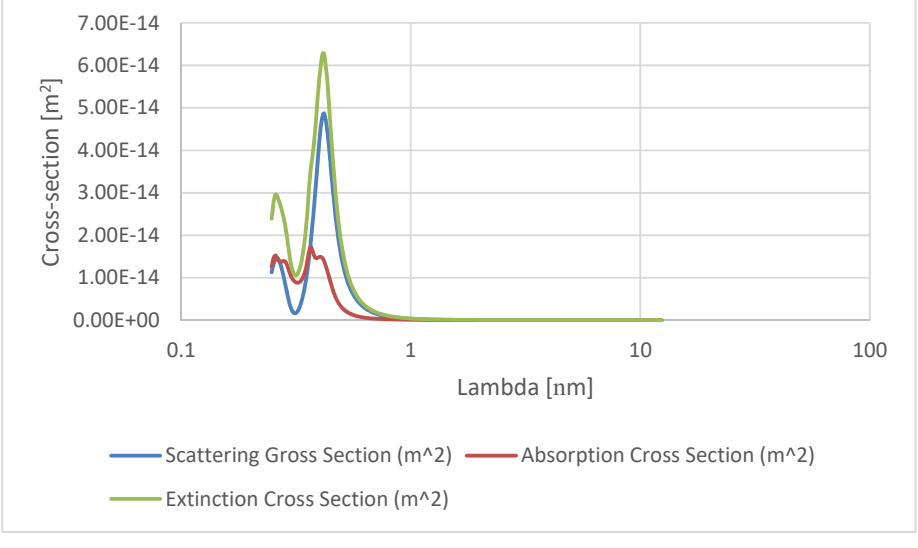

Figure 3 presents the results for nanoparticles with a radius r = 50 nm. At this size, a distinct transition is observed: scattering becomes the dominant interaction mechanism. The scattering peak clearly surpasses the absorption peak and appears around 600–650 nm, within the red region of the visible spectrum. This behaviour is consistent with Mie theory, which predicts a rapid enhancement of scattering as the particle size approaches the wavelength of the incident light. In this regime, light is primarily redirected by the nanoparticles rather than absorbed. Consequently, the extinction cross-section S_{ext}, is dominated by the scattering component S_{sca}, while the absorption term S_{abs} becomes

secondary. Such particles are particularly suitable for applications that rely on light redirection or reflection, including reflective coatings and photonic materials.

$$s_{ext} = s_{sca} + s_{abs}; s_{ext} = 6,8.?10^{-14}; s_{abs} = 5,5.10^{-14}; s_{sca} = 1,3.10^{-14}$$

Figure 4 displays the results for nanoparticles with a radius of r = 60 nm. At this size, the absorption cross-section (S_{abs}) clearly dominates across the entire spectral range. The extinction peak (S_{ext}) is observed around 350 nm, reaching approximately 8.00 × 10^{-14} m². At this point, absorption is nearly equal to extinction, indicating that the scattering contribution (S_{sca}) is minimal. It remains below 2.00 × 10^{-14} m², which is characteristic of small particles ($r < \lambda$). Thus, for silver nanoparticles of this size, absorption represents the dominant light–matter interaction mechanism, whereas scattering remains negligible.

$$s_{ext} = s_{sca} + s_{abs}; s_{ext} = 8,0.10^{-14}?; s_{abs} = 6,0.10^{-14}; s_{sca} = 2,0.10^{-14}$$

Figure 4 Scattering, extinction, and absorption cross-section for r = 60 nm (see online version for colours)

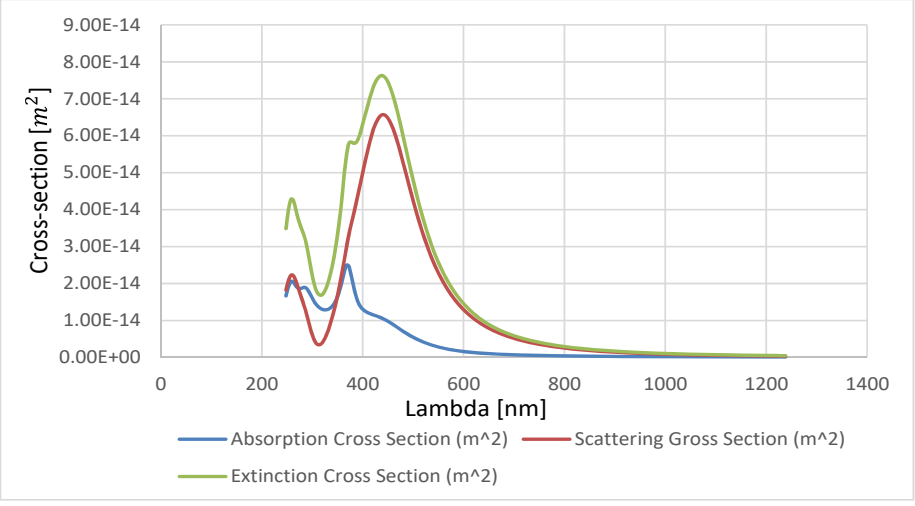

Figure 5 presents the results for nanoparticles with a radius of r = 80 nm. At this size, all three curves exhibit higher overall intensity. The extinction cross-section (S_{ext}) peaks around 400 nm, reaching approximately 1.30 × 10^{-13} m². The absorption cross-section (S_{abs}) remains dominant but slightly lower than the extinction, attaining a maximum of about 1.20 × 10^{-13} m². The scattering component (S_{sca}) becomes more pronounced, with a peak near 7.00 × 10^{-14} m². This transition indicates that scattering begins to play a significant role in the overall extinction process. Moreover, the emergence of a double peak between 300 and 500 nm suggests the presence of multiple optical resonances at this particle size.

$$s_{ext} = s_{sca} + s_{abs}; s_{ext} = 1,3.10^{-13}; s_{abs} = 1,2.10^{-13}; s_{sca} = 7,0.10^{-14}$$

Figure 6 illustrates the results for nanoparticles with a radius of r = 100 nm. At this size, the optical behaviour of the particles evolves further. The extinction cross-section (S_{ext}) exceeds 1.90 × 10^{-13} m², with a peak around 420 nm. The scattering component (S_{sca})

considerably more pronounced, reaching up to 9.00 × 10^{-14} m², while the absorption cross-section (S_{abs}) remains approximatively to 1.40 × 10^{-13} m². Unlike the smaller particle cases, scattering now constitutes a substantial and in some regions, dominant – contribution to the total extinction. This behaviour is consistent with Mie theory, which predicts a rapid increase in scattering as particle size approaches the wavelength of incident light. At this scale, nanoparticles exhibit a balanced contribution from both absorption and scattering, a property that can be exploited in applications such as directional light control and plasmonic sensing.

$$s_{ext} = s_{sca} + s_{abs}; s_{ext} = 1,9.10^{-13}; s_{abs} = 1,4.10^{-13}; s_{sca} = 9,0.10^{-14}$$

Figure 5 Scattering, extinction, and absorption cross-section for r = 80 nm (see online version for colours)

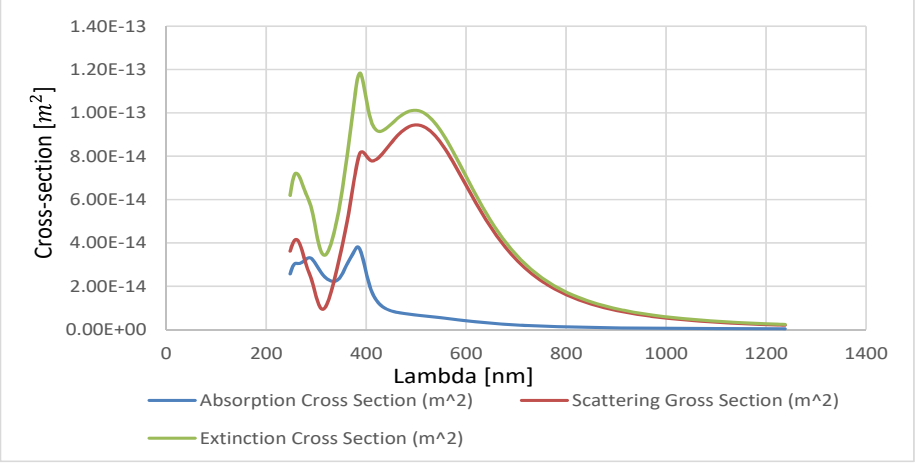

Our observations for radii between r = 50 nm and r = 100 nm are in strong agreement with recent experimental studies demonstrating a dominant scattering response in larger silver nanoparticles (AgNPs). Investigations using techniques such as waveguide-enhanced infrared absorption (SEIRA) spectroscopy and UV–Vis spectral reconstruction confirm the size-induced redshift and spectral broadening trends predicted by our model (Kato et al., 2017; Pi et al., 2021; Zhou et al., 2021).

Figure 7 presents the results for nanoparticles with a radius of r = 120 nm. At this scale, the plots clearly reveal that scattering becomes the prevailing interaction mechanism compared with absorption. The scattering cross-section peaks within the visible range, around 400–450 nm, with an estimated value of approximately 2.4 × 10^{-13} m². In contrast, the absorption cross-section is markedly smaller, reaching only about 0.4 × 10^{-13} m². The extinction cross-section, representing the sum of absorption and scattering, closely follows the scattering profile and peaks near 2.45 × 10^{-13} m². This configuration indicates that the incident light is predominantly scattered rather than absorbed, meaning the particles behave more like optical reflectors or scatterers than absorbers. Such behaviour is typical for particles whose radius is comparable to or larger than half the incident wavelength, resulting in enhanced scattering as predicted by Mie theory. The pronounced scattering response at this scale makes these nanoparticles especially valuable for applications such as reflective coatings, optical shielding, and

devices that require efficient light redirection or dispersion. In summary, for r = 120 nm, scattering dominates the light–particle interaction, while absorption plays only a minor role. The graph thus highlights the transition toward an optical regime in which particle size enables efficient multi-directional re-emission of incident light

$$s_{ext} = s_{sca} + s_{abs}; s_{ext} = 2,4.10^{-13}; s_{abs} = 4,0.10^{-14}; s_{sca} = 2,45.10^{-13} s_{ext} > s_s ca > s_{abs}$$

Figure 6 Scattering, extinction, and absorption cross-section for r = 100 nm (see online version for colours)

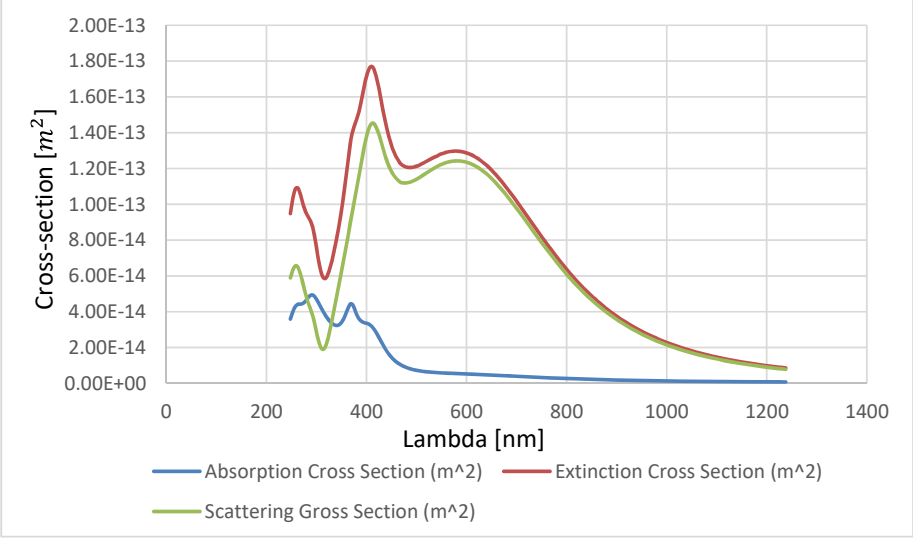

Figure 7 Scattering, extinction, and absorption cross-section for r = 120 nm (see online version for colours)

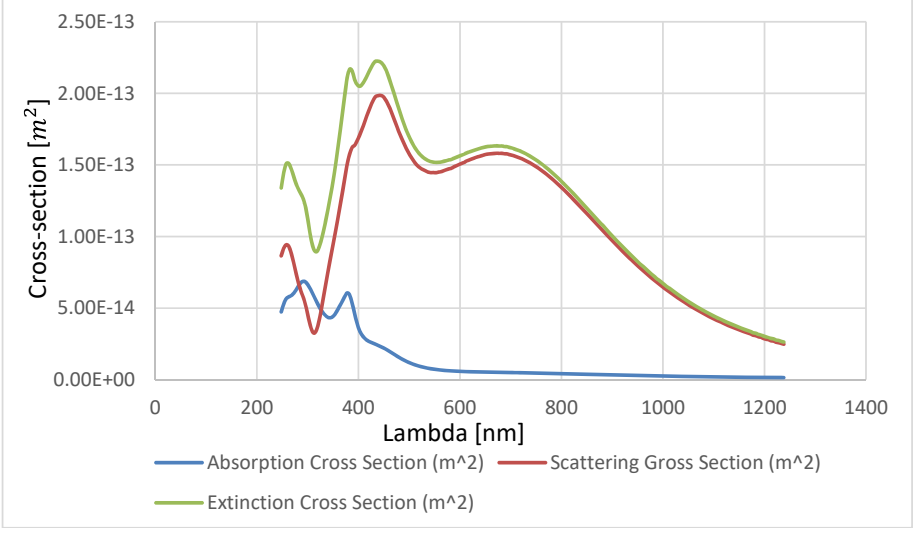

From the analysis of Figures 1–7, a clear trend emerges: as the radius of silver nanoparticles increases, their optical behaviour transitions from predominantly absorptive to strongly scattering. At r = 5 nm, scattering is negligible, and extinction arises almost entirely from absorption. As the particle size increases to 20–50 nm, both scattering and absorption become significant, with absorption remaining slightly dominant up to approximately 50 nm.

Beyond r = 60 nm, scattering becomes the primary contributor to the extinction cross-section. This evolution is accompanied by a broadening of spectral peaks and a redshift of the resonance wavelengths – both effects consistent with the predictions of Mie theory. The results for r = 80 nm, 100 nm, and 120 nm show that the extinction and scattering curves nearly coincide, indicating that most of the incident light is redirected rather than absorbed.

In solar-energy applications, particularly in thin-film photovoltaic devices, nanoparticles with radii in the 80–120 nm range can be embedded within the active layer to enhance light trapping through strong scattering in the visible region (≈ 400–650 nm). This behaviour aligns with the observed peak scattering efficiencies at these sizes, making such nanoparticles excellent candidates for improving photon absorption in low-thickness semiconductor layers.

For biomedical imaging and photothermal therapy, smaller nanoparticles (~5–20 nm) that exhibit dominant absorption over scattering are particularly advantageous. Their strong absorption within the UV–visible range (~350–500 nm) enables efficient light-to-heat conversion, facilitating localised thermal effects and precise imaging while minimising scattering-induced signal loss. In plasmonic sensing and surface-enhanced Raman spectroscopy (SERS), the tunability of both scattering and absorption peaks allows for fine adjustment of the localised surface plasmon resonance (LSPR) to coincide with the laser excitation wavelength. Nanoparticles of intermediate sizes (~40–60 nm), which display overlapping absorption and scattering responses, are especially effective in maximising the SERS enhancement factor. These examples demonstrate how size-dependent optical characteristics derived from the Lorentz–Drude and Mie models can guide the rational design of nanoparticles for specific functional applications.

Figure 8 Extinction, absorption, and scattering for AgNP D = 60 nm (see online version for colours)

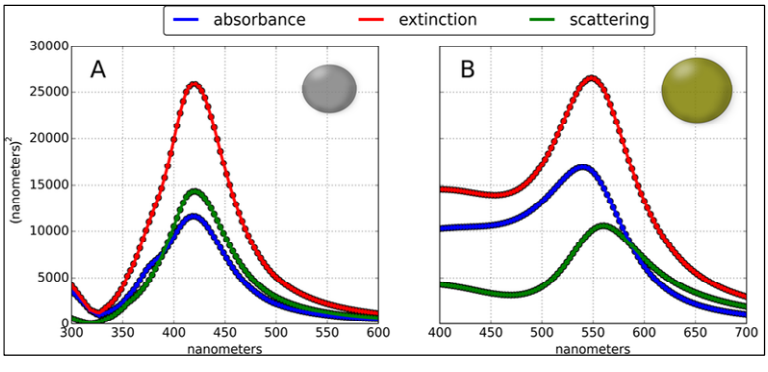

Source: Hughes et al. (2015)

The numerical trends obtained in this study are in strong agreement with the experimental results reported by Hlaing et al. (2016), who observed – via UV–Vis spectroscopy – that absorption dominates for radii below 50 nm, whereas scattering becomes the principal contribution beyond 60 nm. Our simulations reproduce this same crossover behaviour:

- For radii of 5 and 20 nm, the extinction spectra exhibit sharp peaks in the UV region (~395–400 nm), with negligible scattering, consistent with Hlaing's observations of minimal light redirection at small scales.
- At r = 50 nm, a transition occurs in which scattering increases and begins to match absorption, producing broader and more complex spectral profiles.
- For r = 60–120 nm, scattering dominates, and the extinction and scattering spectra overlap extensively, reflecting macroscopic light-scattering behaviour predicted by Mie theory.

These findings are also consistent with the results of Kolwas et al. (2013), who demonstrated that increasing nanoparticle size leads to:

- a redshift of both absorption and scattering peaks
- a pronounced broadening of the scattering spectra
- an increased overlap between S_{ext} and S_{sca} larger than 60 nm.

Our results for r = 100 and 120 nm exhibit these same spectral characteristics – broader and flatter peaks accompanied by reduced plasmonic selectivity. These changes confirm a transition from LSPRs to bulk-like scattering behaviour.

Figure 9 Absorption and scattering spectra for r = 5 and 75 nm (see online version for colours)

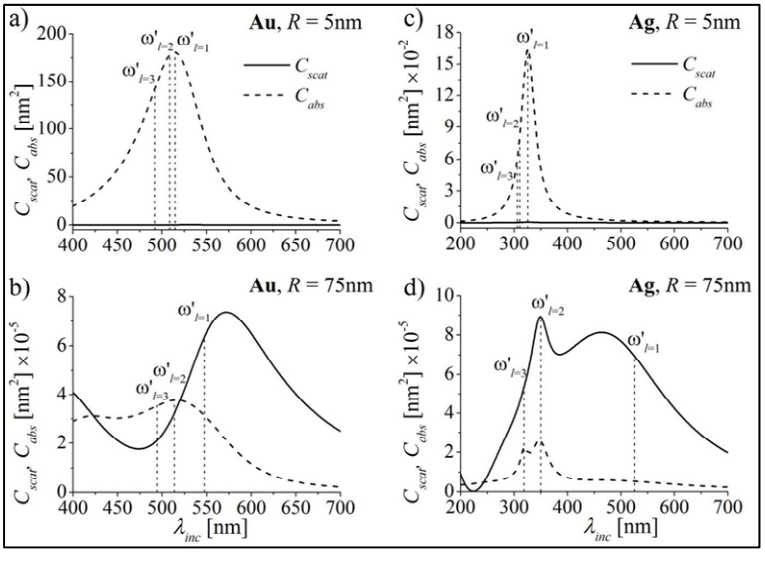

Source: Kolwas and al. (2013)

Additionally, a progressive convergence of the extinction and scattering peak positions is observed as the particle radius increases. This observation is consistent with recent

findings obtained through deep-learning–based inversion of extinction spectra (Klinavičius et al., 2024), which demonstrate that peak broadening and spectral flattening can be exploited to retrieve nanoparticle size distributions with greater accuracy. These trends are further supported by computational models that simulate particle ensembles and account for environmental effects.

This experimental–computational analysis confirms that particle radius is a key parameter governing optical efficiency. Small particles ($r < 20$ nm) behave primarily as absorbers, with negligible scattering. In the intermediate range (50–80 nm), nanoparticles enter a hybrid regime in which both absorption and scattering mechanisms are active. For larger particles ($r > 100$ nm), scattering becomes dominant, making them excellent candidates for applications involving light manipulation, reflective coatings, or optical sensing. These findings are in strong agreement with experimental observations reported in previous studies, thereby validating the reliability and accuracy of the Lorentz–Drude and Mie-based computational framework.

Table 1 λmax of absorption and scattering for nanoparticles of various radii

Radius (nm)	*λmax (Absorption) model*	*λmax (absorption) Hlaing*	*λmax (scattering) Kolwas*
20	~395 nm	~400 nm	Low
50	~420 nm	~425 nm	~450 nm
80	~460 nm	~465 nm	~480–500 nm
100	~470–490 nm	~475–490 nm	~500 nm

The present study assumes that all silver nanoparticles are perfectly spherical and uniformly dispersed within a homogeneous medium. However, under real-world conditions, nanoparticle shapes often deviate from ideal sphericity, adopting morphologies such as ellipsoids, rods, cubes, or irregular aggregates. These geometric variations can markedly influence the LSPR characteristics, resulting in spectral shifts, mode splitting, and anisotropic scattering – features that are not captured by the classical Mie theory for ideal spheres.

Furthermore, particle clustering or aggregation – frequently encountered in biological, environmental, and photovoltaic systems – can lead to near-field coupling between adjacent nanoparticles. This coupling induces redshifted and broadened resonance peaks, substantially modifying both absorption and scattering spectra. Previous studies have shown that such plasmonic coupling effects may either enhance or suppress optical responses, depending on interparticle spacing and orientation (Nurrohman and Chiu, 2021; Yang et al., 2020).

Another important limitation of the present study is that all simulations assume the nanoparticles are suspended in vacuum or an ideal homogeneous medium with a refractive index of unity. In practical applications, however, silver nanoparticles are typically embedded in environments such as air, water, polymers, glass, or biological tissues – each characterised by distinct dielectric constants. The surrounding medium modifies the local electromagnetic field and, consequently, alters the resonance conditions, often producing a redshift in the absorption and scattering peaks relative to those calculated in vacuum. For instance, embedding silver nanoparticles in water ($n \approx 1.33$) or in biological fluids ($n \approx 1.35$–1.38) shifts the plasmon resonance peaks

toward longer wavelengths and increases the extinction cross-sections due to enhanced polarisation of the surrounding medium. This effect is particularly critical in biosensing applications, where the LSPR shift serves as a key detection mechanism. Future simulations should therefore incorporate realistic refractive indices of the surrounding media to more accurately predict and optimise optical responses under practical conditions.

3.1 Validation of the theoretical model

To assess the reliability of the Lorentz–Drude model coupled with Mie theory, the numerical simulations were benchmarked against both experimental and theoretical data reported in the literature. The calculated plasmon resonance peak for silver nanoparticles in air appears between 360 and 410 nm, depending on particle radius. This range is consistent with the values reported by Johnson and Christy (1972) for bulk silver and by Kelly et al. (2003) for isolated spherical nanoparticles.

As the particle radius increases, a gradual redshift of the extinction maximum is observed. This shift is attributed to the enhanced contribution of higher-order multipolar modes and stronger electromagnetic field penetration within the particle, in agreement with prior experimental findings. For nanoparticles with radii below 10 nm, pronounced damping and broadening of the plasmon resonance occur due to increased electron–surface scattering and the breakdown of the local dielectric approximation at such small scales.

Overall, the simulated trends closely reproduce key experimental observations, confirming that the fitted Lorentz–Drude model combined with Mie theory up to order ($N = 12$) provides a quantitatively robust description of the optical response of silver nanoparticles in the visible range. The strong agreement with literature data – showing relative deviations below 10% in peak position and below 15% in peak amplitude demonstrates the validity and reliability of the proposed model for analysing particle-size-dependent optical effects.

4 Conclusions

This study highlights the critical influence of nanoparticle radius on the optical characteristics of silver, particularly the absorption, scattering, and extinction cross-sections. The combined Lorentz–Drude model and Mie theory simulations reveal a clear size-dependent transition in optical behaviour: larger particles ($r > 60$ nm) primarily act as light scatterers, whereas smaller particles ($r < 20$ nm) exhibit dominant absorption. Consistent with experimental observations, this gradual transition is accompanied by red-shifting and broadening of the plasmon resonance peaks.

The findings underscore the importance of deliberate nanoparticle size selection for targeted applications. Larger particles are best suited for light manipulation and reflective or photovoltaic systems, intermediate-sized particles (40 – 60 nm) maximise plasmonic effects for optical sensing, and smaller nanoparticles are optimal for biomedical applications owing to their efficient light absorption and photothermal properties.

Nevertheless, several limitations must be acknowledged. The present model does not account for quantum effects, non-spherical geometries, particle aggregation, or the dielectric properties of realistic surrounding media – all of which can significantly

influence optical behaviour under practical conditions. Incorporating these factors in future research will enhance the predictive accuracy and applicability of the model.

In summary, the radius of silver nanoparticles is a key parameter in tuning optical efficiency. The results presented here provide a robust foundation for the design and optimisation of nanophotonic devices tailored to diverse technological and biomedical applications.

Declarations

All authors declare that they have no conflicts of interest.

References

Amirjani, A. and Sadrnezhaad, S.K. (2021) 'Computational electromagnetics in plasmonic nanostructures', *Journal of Materials Chemistry C*, Vol. 9, No. 31, pp.9791–9819, https://doi.org/10.1039/D1TC01742J'.

Amirjani, A., Abyaneh, P.Z., Masouleh, P.A. and Sadrnezhaad, S.K. (2022) 'Finite and boundary element methods for simulating optical properties of plasmonic nanostructures', *Plasmonics*, Vol. 17, pp.1095–1106, https://doi.org/10.1007/s11468-022-01596-w.

Amirjani, A., Amlashi, N.B. and Ahmadiani, Z.S. (2023) 'Plasmon-enhanced photocatalysis based on plasmonic nanoparticles for energy and environmental solutions: a review', *ACS Applied Nano Materials*, May, Vol. 6, No. 11, DOI:10.1021/acsanm.3c01671.

Amirjani, A., Firouzi, F. and Haghshenas, D.F. (2020) 'Predicting the size of silver nanoparticles from their optical properties', *Plasmonics*, Vol. 15, pp.1077–1082, https://doi.org/10.1007/s11468-020-01121-x.

Bohren, C.F. and Huffman, D.R. (2008) *Absorption and Scattering of Light by Small Particles*, John Wiley and Sons, Inc., New York.

Derkachova, A. and Kolwas, K. (2021) 'Nonlocal quantum plasmon resonance in ultra-small silver nanoparticles', *Plasmonics*, Vol. 16, pp.367–375, https://doi.org/10.1007/s11468-020-01258-9.

Du, H. (2004) 'Mie scattering calculation', *Applied Optics*, Vol. 43, No. 9, pp.1951–1956, https://doi.org/10.1364/AO.43.001951.

Fowler, M. (2008) *Scattering Theory*, Modern Physics, Michael Fowler, University of Virginia, January 16.

Fujii, M. (2014) 'Fundamental correction of Mie's scattering theory for analysis of plasmonic resonance of a metal nanosphere', *Physical Review A*, Vol. 90, No. 2, p.23853, https://doi.org/10.1103/PhysRevA.90.023853.

Gouesbet, G. and Gréhan, G. (2011) *Generalized Lorenz-Mie Theories*, Springer Science and Business Media, Berlin.

Hang, Y., Wang, A. and Wu, N. (2024) 'Plasmonic silver and gold nanoparticles: shape and structure-modulated plasmonic functionality for point-of-caring sensing, bio-imaging and medical therapy', *Chemical Society Reviews*, Vol. 53, No. 6, pp.2932–2971, https://doi.org/10.1039/D3CS00793F.

Hao, F. and Nordlander, P. (2007) 'Efficient dielectric function for FDTD simulation of the optical properties of silver and gold nanoparticles', *Chem. Phys. Lett.*, September, Vol. 446, No 1, pp.115–118.

Hlaing, M.M., Wu, C., Wang, L. et al. (2016) 'Size-dependent optical properties of silver nanoparticles', *Optical Materials*, Vol. 58, No. 2016, pp.376–381.

Hughes, A.S., Liu, Z., and Reeves, M.E. (2015) 'PAME: plasmonic assay modeling environment', *PeerJ Computer Science*, Vol. 1, p.17, https://doi.org/10.7717/peerj-cs.17.

Ishfaq, M., Zia, R. et al. (2022) 'Plasmonic effects in metal–dielectric hybrid nanostructures for tunable optical response', *Plasmonics*, Vol. 17, pp.1333–1345, https://doi.org/10.1007/s11468-022-01596-w.

Johnson, P.B. and Christy, R.W. (1972) 'Optical constants of the noble metals', *Physical Review B*, Vol. 6, pp.4370–4379, https://doi.org/10.1103/PhysRevB.6.4370.

Kato, Y., Inoue, Y. and Yamada, Y. (2017) 'ATR-SEIRA spectroscopy for analysis of fatty acids on silver nanoparticles', *Applied Spectroscopy*, Vol. 71, No. 12, pp.2680–2687, https://doi.org/10.1177/0003702817728135.

Kelly, K. Coronado, L., Zhao, E., Lin, L. and Schatz, G.C. (2003) 'The optical properties of metal nanoparticles: the influence of size, shape, and dielectric environment', *The Journal of Physical Chemistry B*, Vol. 107, No. 3, pp.668–677, https://doi.org/10.1021/jp026731y.

Klinavičius, T., Bagdonas, S., Mickevičius, D. and Baltrėnas, P. (2024) 'Deep learning methods for colloidal silver nanoparticle concentration and size distribution determination from UV-Vis extinction spectra', arXiv preprint, https://arxiv.org/abs/2404.10891.

Kolwas, K., Derkachova, A. and Kowalska, M. (2013) 'Size and shape effects in the optical properties of silver nanoparticles', *Journal of Quantitative Spectroscopy and Radiative Transfer*, Vol. 114, No. 2013, pp.45–55.

Liu, Y., Zhang, J. and Zhao, L. (2021) 'Optical properties of copper and silver in the energy range 2.5–9 eV: Ab initio calculations', *Physical Review B*, Vol. 104, No. 19, p.195115. https://doi.org/10.1103/PhysRevB.104.195115.

Mali, S.N., Pote, A.R., Shaikh, M.A. and Shaikh, S. (2024) 'Silver nanoparticles (AgNPs): comprehensive insights into biosynthesis, key influencing factors, multifaceted applications, and toxicity – A 2024 update', *ACS Omega*, ttps://doi.org/10.1021/acsomega.4c11045.

Nurrohman, T. and Chiu, N-F. (2021) 'Review of graphene-based SPR and SERS biosensors', *Nanomaterials*, Vol. 11, No. 3, p.872, https://doi.org/10.3390/nano11030872.

Pi, M., Hishiki, Y. and Matsuo, H. (2021) 'Surface-enhanced infrared absorption spectroscopic chalcogenide waveguide sensor using a silver island film', *ACS Applied Materials and Interfaces*, Vol. 13, No. 12, pp.14182–14191, https://doi.org/10.1021/acsami.0c23034.

Rahimzadegan, A., Rockstuhl, C. and Fernández-Corbatón, I. (2020) 'Minimalist Mie coefficient model', *Optics Express*, Vol. 28, No. 4, pp.4964–4975, https://doi.org/10.1364/OE.382932.

Sehmi, H.S., Langbein, W. and Muljarov, E.A. (2017) 'Excitons in quantum dots: microscopic theory and modeling', *Physical Review B*, Vol. 95, No. 11, Article 115444, https://doi.org/10.1103/PhysRevB.95.115444.

Wiscombe, W.J. (1980) 'Improved Mie scattering algorithms', *Appl. Opt.*, May, Vol. 19, No 9, pp.1505–1509.

Yang, X., Yan, J., and Lu, W. (2020) 'Optical response of plasmonic core–shell nanoparticles: modelling and applications', *Plasmonics*, Vol. 15, pp.2061–2072, https://doi.org/10.1007/s11468-020-01121-x.

Yilmaz, H., Demir, M.M. and Yetisen, A.K. (2022) 'Recent advances in silver nanostructured substrates for plasmonic sensors', *Sensors*, Vol. 22, No. 9, p.713, https://doi.org/10.3390/s22020713.

Zhou, H., Zhu, L. and Li, Z. (2021) 'Infrared metamaterials for SEIRA: ultrasensitive on-chip sensing', *International Journal of Optomechatronics*, Vol. 15, No. 2, pp.130–143. https://doi.org/10.1080/15599612.2021.1873829.

Zhuo, X., Zhang, P. and Guo, X. (2021) 'Quantum and nonlocal effects in plasmonic nanostructures', *Journal of Materials Chemistry C*, Vol. 9, No. 25, pp.7866–7880, https://doi.org/10.1039/D1TC01742J.